ELSEVIER

Biochimica et Biophysica Acta 1205 (1994) 268–274

BBA Biochimica et Biophysica Acta

Analysis of progress curves for enzyme-catalyzed reactions: application to unstable enzymes, coupled reactions and transient-state kinetics

Ronald G. Duggleby *

Centre for Protein Structure, Function and Engineering, Department of Biochemistry, University of Queensland, Brisbane, Qld. 4072, Australia

(Received 16 August 1993)

Abstract

There are several advantages to the use of progress curves to analyze the kinetic properties of enzymes but most studies still rely on rate measurements. One of the reasons for this may be that progress curve analysis relies on the enzyme and the reactants being completely stable under assay conditions. Here a method is described that relaxes this requirement and allows progress curve analysis to be applied to unstable enzymes. The procedure is based on a combination of numerical integration and non-linear regression to fit rate equations to the progress curve data. The analysis is verified using simulated data and illustrated by application to the reaction catalyzed by alkaline phosphatase, measured in the presence of 10 mM EGTA where it has a half-life of $3\frac{1}{2}$ min. The method may also be applied to other experimental systems where the development over time reveals important properties but where an analytical solution of the underlying model is not known. This extension is illustrated by two systems: the coupled reactions catalyzed by pyruvate kinase and lactate dehydrogenase under conditions where both enzymes have similar activity; and the transient-state kinetics of the reaction catalyzed by glutamate dehydrogenase.

Key words: Enzyme-catalyzed reaction; Progress curve; Transient-state kinetics; Enzyme; Coupled reaction

1. Introduction

In almost any kinetic experiment on an enzyme-catalyzed reaction there is a fundamental incompatibility between the data and the underlying model. This is because most kinetic models are formulated in terms of *rates* of reaction while the usual way in which the reaction is monitored is by measuring the *amount* of reactant remaining or product formed at one or more times. To resolve this incompatibility, either the model must be integrated to give a description of the time course of the reaction or the data must be differentiated by measuring tangents to the reaction progress curves, thereby determining rates.

Traditionally, enzyme kinetic studies have employed the second approach and have focussed on determining rates, especially initial rates, but there are advantages with each approach. First, if initial rates are measured, the substrate concentration is exactly equal to that which is added. However, in the reaction progress curve the substrate concentration is automatically varied as the reaction proceeds providing information about the dependence upon substrate concentration of the enzyme. Secondly, for initial rates, there is a vanishingly small concentration of potentially inhibitory reaction products present, unless these are added deliberately. On the other hand, products of the correct stereochemistry and of complete purity are formed automatically in a progress curve as the reaction proceeds, providing information about the dependence upon product concentration of the enzyme. As a consequence of the above, considerably more information is obtained from each assay if the entire progress curve is analyzed and a complete description of the kinetic properties of the enzyme can be obtained from fewer experiments.

Given these advantages, one may enquire why all enzyme kinetic studies do not exploit progress curves. Until fairly recently, one of the main reasons was probably that the data analysis is considerably more complex than that for rate measurements. While simple graphical methods may suffice in some instances

* Corresponding author. E-mail: duggleby@biosci.uq.oz.au. Fax: +61 7 3654699.

SSDI 0167-4838(93)E0245-W

(see Ref. 1 for review), most systems require non-linear regression analysis of the data. This approached was pioneered by Nimmo and Atkins [2] and by Fernley [3], and involves deriving the integrated rate equation then incorporating this into a suitable non-linear regression analysis computer program. A few years ago we [4] developed a procedure based on the work of Boeker [5–7] that greatly simplifies the analysis. This procedure took advantage of the fact that the process of going from a differential rate equation to a functioning non-linear regression program is a largely mechanical, but tedious and error-prone, process; as such it lent itself to automation. Knowing only the differential rate equation for a particular mechanism, which have been extensively catalogued (e.g., see Ref. 8), it is now possible to analyze the progress curves of most enzyme-catalyzed reactions.

There is a second reason that progress curve analysis may not be widely used. In some cases the shape of the progress curve may not depend solely upon the variations in reactant concentrations that are due to the catalyzed reaction. The enzyme may undergo a progressive inactivation, or some of the reactants may undergo side reactions. While there is a simple test to detect such problems [9], they are not easily overcome. By contrast, progressive loss of enzyme activity or reactants have relatively little influence when initial rates are measured.

It is unfortunate that the advantages of progress curve analysis are lost when there is instability of the enzyme and we have tried previously to overcome this limitation [10,11]. It was shown theoretically and verified in practice that progress curves could be used in these circumstances. From the residual substrate concentration after prolonged incubation it is possible to determine the inactivation rate constants of various complexes along the catalytic pathway. Unfortunately, the normal kinetic constants (maximum velocity, Michaelis constants and inhibition constants) are not obtained readily from the data.

Here a new analysis is developed that will allow progress curves to be used for kinetic characterization of an unstable enzyme. The method is also shown to be useful for simultaneous kinetic characterization of two or more enzymes in a coupled systems, and for analysis of transient-state kinetics.

2. Theory

Scheme 1 shows the simplest case of an unstable enzyme. There is only one substrate and the reaction is irreversible, producing a non-inhibitory product. The free enzyme and the enzyme-substrate complex are each unstable being converted to the inactive forms F_1 and F_2 with rate constants of j_1 and j_2, respectively.

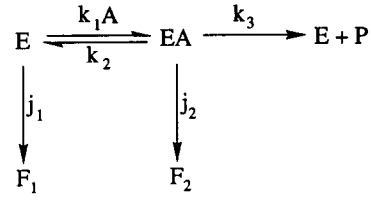

Scheme 1.

The kinetics of this system are described by two differential equations describing the rate of loss of active enzyme $[E']_t$ and the rate of utilization of substrate $[A]_t$.

$$\frac{d[E']_t}{dt} = \frac{-[E']_t(j_1 + j_2[A]_t/K_a)}{1 + [A]_t/K_a} \quad (1)$$

$$\frac{d[A]_t}{dt} = \frac{-k_3[E']_t[A]_t/K_a}{1 + [A]_t/K_a} \quad (2)$$

If we are to apply progress curve analysis to this system we must be able to calculate $[A]_t$ at any time. These values are compared with the experimental values and, by non-linear regression, used to obtain best fit values for the various parameters (j_1, j_2, k_3 and K_a,). It will be noted that these differential equations are coupled; that is to obtain an expression for $[E']_t$ from Eq. (1) requires a knowledge of $[A]_t$ while to obtain an expression for $[A]_t$ from Eq. (2) requires a knowledge of $[E']_t$. Except in some special cases (e.g., when j_1 is equal to zero or to j_2) these equations cannot be solved algebraically.

They can, however, be solved numerically; given particular values of the parameters, as well as defined starting conditions ($[E']_0$ and $[A]_0$), Eqs. (1) and (2) can be evaluated. These rates are applied over a small time interval to calculate $[E']_t$ and $[A]_t$ after this time. The process is then repeated as often as required to obtain the entire progress curve for substrate utilization.

This is a relatively crude method and more sophisticated algorithms have been described [12]. The method selected for the present work is the 3rd and 4th order Runge–Kutta–Fehlberg procedure with automatic step size control. By incorporating this numerical integration algorithm into the DNRP53 computer program [13] we are able to analyze reaction systems described by coupled differential equations.

We have used three experimental systems to evaluate the method. The first is an unstable enzyme, bovine intestinal mucosal alkaline phosphatase. This is a slightly more complex system than Scheme 1 because the enzyme is inhibited by one of its products, phosphate ion. Although the enzyme is normally quite stable, the essential zinc ion can be removed by EGTA leading to inactivation. However, only the free enzyme is susceptible to this effect; in the enzyme-substrate

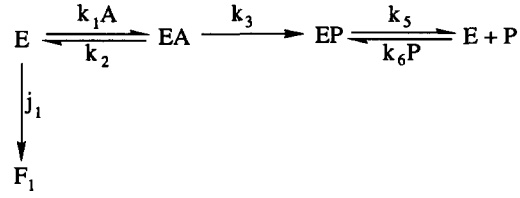

Scheme 2.

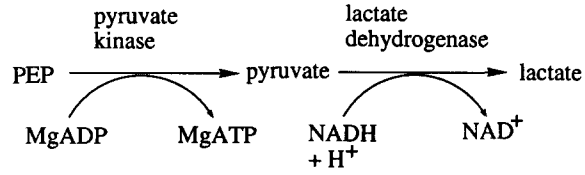

Scheme 3.

complex the zinc is locked in, as it is in the enzyme-phosphate complex. The system is described by Scheme 2 and Eqs. (3) and (4).

$$\frac{d[E']_t}{dt} = \frac{-j_1[E']_t}{1 + [A]_t/K_a + [P]_t/K_p} \quad (3)$$

$$\frac{d[P]_t}{dt} = \frac{k_3[E']_t[A]_t/K_a}{1 + [A]_t/K_a + [P]_t/K_p} \quad (4)$$

The second experimental system is the coupled reactions catalyzed by pyruvate kinase and lactate dehydrogenase (Scheme 3). Under the experimental conditions selected, none of the potential product or dead-end inhibitions has any significant effect and the concentration of MgADP is sufficiently high that it remains constant for all practical purposes. The system is shown in Scheme 3 and is defined by Eqs. (5) and (6).

$$\frac{d[NAD^+]_t}{dt} = \frac{V_m^{LDH}[pyr]_t[NADH]_t}{[pyr]_t(K_m^{NADH} + [NADH]_t) + K_m^{pyr}(K_i^{NADH} + [NADH]_t)} \quad (5)$$

$$\frac{d[pyr]_t}{dt} = \frac{V_m^{PK}[PEP]_t}{K_m^{PEP} + [PEP]_t} - \frac{d[NAD^+]_t}{dt} \quad (6)$$

The third experimental system is the pre-steady state time domain of the reaction catalyzed by bovine liver glutamate dehydrogenase [14]. The data are described by the model shown in Scheme 4, where A, B and P represent $NADP^+$, glutamate and NADPH, respectively. The conversion of EA to EAB is not explicitly shown because glutamate was present at a very high and constant concentration. The system is described by Eqs. (7)–(9) and the experimental measurements are an estimate of the sum of free and bound NADPH (i.e., $[EP]_t$ plus $[P]_t$).

$$d[EAB]_t/dt = k_1[E]_t[A]_t + k_4[EP]_t - (k_2 + k_3)[EAB]_t \quad (7)$$

$$d[EP]_t/dt = k_3[EAB]_t - (k_4 + k_5)[EP]_t \quad (8)$$

$$d[P]_t/dt = k_5[EP]_t \quad (9)$$

3. Materials and methods

Experimental procedures

Progress curves for alkaline phosphatase were as described previously [11]. Briefly, enzyme (141 to 1128 μg/ml) was added to 3 ml reaction mixtures containing 4-nitrophenyl phosphate (2 to 10 mM) and 10 mM EGTA in 0.15 M Na_2CO_3 buffer, pH 10.0. The formation of the 4-nitrophenolate ion was followed at 479 nm and 30° using a Perkin-Elmer Lambda 3 spectrophotometer.

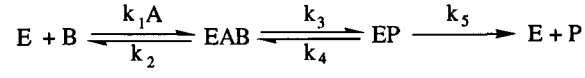

Scheme 4.

```
2000 REM The following statements define some initial quantities
2001 M = 4:    'The number of parameters
2010 N4 = 1:   'The number of independent variables (other than time)
2020 Q = 2:    'The number of differential equations
2030 F1 = 1:   'The fitted variable


5010 REM Define the differential equations here as functions of:
5020 REM    Y(1),Y(2), etc., the dependent variables
5030 REM    X(1),X(2), etc., a series of independent variables
5040 REM    B(1),B(2), etc., the parameters to be fitted
5050 REM    T (time)
5060 REM    D(1) = f(Y(1),Y(2) ...; X(1),X(2) ... ; T)
5070 REM    D(2) = f(Y(1),Y(2) ...; X(1),X(2) ... ; T)
5080 REM    etc.
5090 REM-------------------------------------------------------------------
5100 G1 = X(1) - Y(1):                          [P]t
5110 G2 = 1 + G1 / B(2) + Y(1) / B(3):          Denominator of differentials
5120 D(1) = B(1) * Y(2) * (G1 / B(2)) / G2:     d[P]t/dt
5130 D(2) = -B(4) * Y(2) / G2:                  d[E']t/dt
```

Fig. 1. Sections of the BASIC program defining Eqs. (3) and (4). Lines 2001 to 2030 set some constants associated with the model while lines 5100 to 5130 represent the differential equations themselves.

Pyruvate kinase/lactate dehydrogenase progress curves were as described previously [15]. Reactions were performed at 30° in 0.1 M potassium-Tes buffer (pH 7.5) containing 5 mM ADP, 10 mM $MgCl_2$ and 6.4 mM $(NH_4)_2SO_4$. Assays (3 ml), which contained 40.5 to 446.9 μM PEP, 48.6 to 388.5 μM NADH, 1.639 μg pyruvate kinase and 0.828 μg lactate dehydrogenase, were followed at 360 nm using a Perkin-Elmer Lambda 3 spectrophotometer.

Transient-state kinetics of glutamate dehydrogenase were taken from Fig. 1 of Chandler et al. [14]; the data concern NADPH formation during the first 200 ms of the reaction. Reactions were started by mixing 18 μM enzyme with a mixture of 25 mM glutamate, $NADP^+$ (1250, 240 or 80 μM), 0.2 M NaCl and 0.1 mM EDTA in 50 mM potassium phosphate buffer (pH 7.5).

Data analysis

DNRP53 [13] is a general non-linear regression program, written in BASIC, that can be used for a wide variety of data analysis problems. The program has been modified by inclusion of a numerical integration routine that is a BASIC translation of the Runge–Kutta–Fehlberg algorithm taken from the FORTRAN program, CRICF [14]. In addition, the data input and certain internal features of DNRP53 were modified to tailor the program to the particular nature of progress curve analysis. The resulting program is referred to as DNRP-RKF (copies are available from the author).

To illustrate how the program is adapted to fit a particular set of differential equations, alkaline phosphatase will be used as an example. The relevant part of the program is shown in Fig. 1

First some details of the equations are specified in lines 2001–2030. These are: (a) the number of fitted parameters (four— k_3, K_a, K_p and j_1); (b) the number of independent variables (one—$[A]_o$); (c) the number of differential equations (two —Eqs. (3) and (4)); and (d) the fitted variable (one—i.e., the variable defined by the first differential equation, $[P]_t$).

Lines 5100–5130 the define the differential equations themselves. First, $[P]_t$ (line 5100) and the denominator of Eqs. (3) and (4) (line 5110) are calculated. These are then used in the definitions of $d[P]_t/dt$ (line 5120) and $d[E']_t/dt$ (line 5130).

To speed up the data analysis, the program was compiled using the Microsoft BASIC Professional Development System (version 7.1). The resulting program was run on an IBM-compatible computer.

Simulated data

In Scheme 1, if j_1 is equal to j_2, then Eqs. (1) and (2) can be integrated analytically to give Eq. (10).

$$k_3[E']_o\{1 - \exp(-j_1 t)\}/j_1 = [P]_t - K_a \ln(1 - [P]_t/[A]_o) \quad (10)$$

Given values for $k_3[E']_o$ (which will henceforth be designated as V_m), K_a, j_1 and $[A]_o$, it is possible to solve Eq. (10) and thereby calculate $[P]_t$ at any time t.

A simulated curve was calculated as follows. First, V_m and K_a were given arbitrary values of unity; this involves no loss of generality since these parameters simply define the scale of the time and concentration axes. Second, for a given $[A]_o$, the expected time for $[P]_t/[A]_o = 0.1$, 0.2, and so on up to 0.9 was calculated for the case where there is no enzyme inactivation by replacing the left hand side of Eq. (10) with $V_m t$. Third, from these time values, the expected $[P]_t$ was calculated for a chosen value of j_1 using Eq. (10). Finally, proportional noise was added to these expected values of $[P]_t$ by multiplying by a value chosen randomly from a Gaussian distribution with a mean of 1.0 and particular standard deviation.

Eight sets of curves were calculated, using j_1 values of 0.03, 0.1, 0.2 and 0.35 using both 1% and 5% noise levels. Each set was composed of four curves at $[A]_o$ values of 0.5, 1.0, 2.0 and 5.0. Each set of four curves was then fitted to Eqs. 1 and 2 using DNRP-RKF as described above to obtain values for V_m, K_a and j_1. This entire simulation and fitting was repeated 100 times for each of the eight sets.

4. Results

The results of fitting Eqs. (1) and (2) to the simulated data are summarized in Table 1. When no random error was included, the fitted values of V_m, K_a and j_1 were identical to those used to generate the data. As expected, inclusion of 1% or 5% noise gave values for the fitted parameters that differed somewhat from the theoretical values. However, the means of the fitted values of V_m, K_a and j_1 from the 100 simulations were not significantly different from those used generate the data in all cases.

Table 1
Analysis of simulated data using Scheme 1

j_1	Error (%)	V_m	K_a	j_1
0.03	1	1.0003 ± 0.0070	1.0010 ± 0.0114	0.0304 ± 0.0032
0.03	5	0.9966 ± 0.0326	1.0023 ± 0.0586	0.0324 ± 0.0164
0.10	1	0.9997 ± 0.0070	0.9998 ± 0.0120	0.1000 ± 0.0029
0.10	5	1.0021 ± 0.0300	1.0100 ± 0.0547	0.1032 ± 0.0148
0.20	1	0.9991 ± 0.0067	0.9990 ± 0.0108	0.1999 ± 0.0035
0.20	5	1.0016 ± 0.0362	1.0171 ± 0.0596	0.2018 ± 0.0177
0.35	1	1.0000 ± 0.0063	1.0013 ± 0.0100	0.3497 ± 0.0038
0.35	5	0.9955 ± 0.0354	1.0055 ± 0.0576	0.3484 ± 0.0184

Data were generated as described in the text using values for V_m and K_a of 1.0, and values for j_1 and the percent error shown in the first two columns. The final three columns show the means and standard deviations of values obtained by fitting Eqs. (1) and (2) to 100 simulations.

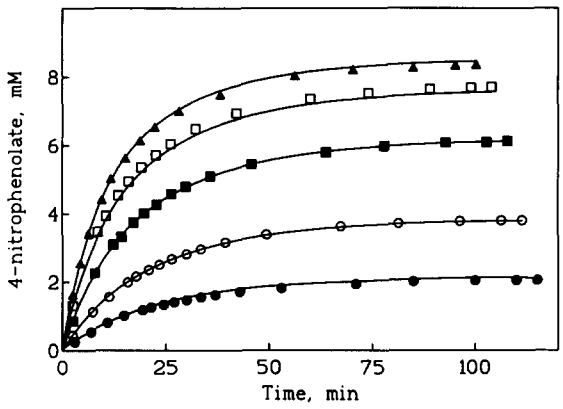

Fig. 2. Progress curves for the hydrolysis of 4-nitrophenyl phosphate, catalyzed by alkaline phosphatase. The data were obtained at enzyme concentrations (top to bottom) of 1128, 846, 564, 282 and 141 μg/ml using an initial substrate concentration of 10 mM.

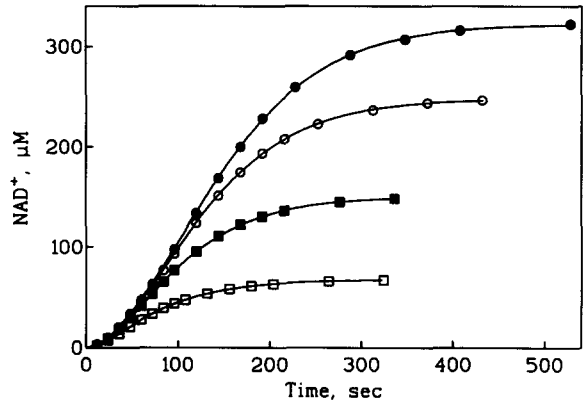

Fig. 3. Progress curves for the coupled reactions catalyzed by pyruvate kinase and lactate dehydrogenase. Reactions were as described in the text with an initial NADH concentration of 386.1 μM and initial PEP concentrations (top to bottom) of 322.6, 247.9, 150.7 and 68.0 μM.

Some representative progress curves for the hydrolysis of 4-nitrophenyl phosphate are shown in Fig. 2. Fitting Eqs. (3) and (4) to these data gave the results shown in Table 2; the kinetic parameters are in excellent agreement with those obtained previously and, as shown by the curves in Fig. 2, describe the data quite well. Further analysis of these data was undertaken by including the added possibility that either EA or EP (Scheme 1) might be unstable. For EP, a value of $(1.834 \pm 1.169) \cdot 10^{-3}$ min^{-1} was obtained for the inactivation rate constant. This is 100 times less than j_1 and corresponds to a half-life of 378 min which three times longer than the maximum incubation time employed. An F-test [16] showed no significant improvement in the overall fit upon inclusion of this additional route of enzyme inactivation. Allowing for EA inactivation gave a negative value for the rate constant ($(-2.492 \pm 10.251) \cdot 10^{-3}$ min^{-1}) and again the F-test indicated no significant improvement in the overall fit.

Table 2
Comparison of results from the present analysis with those in the literature

Parameter	This study	Literature value
Alkaline phosphatase [a]		
k_3 (mmol min^{-1} mg^{-1})	0.871 ± 0.020	0.878 ± 0.021 [b]
K_a (mM)	2.58 ± 0.20	2.70 ± 0.14 [b]
K_p (mM)	1.91 ± 0.15	2.10 ± 0.18 [b]
		2.25 ± 0.06 [c]
j_1 (min^{-1})	0.196 ± 0.011	0.209 ± 0.004 [c]
		0.196 ± 0.007 [d]
Pyruvate kinase [e]		
V_m^{PK} (U mg^{-1})	370 ± 2	370 ± 3 [f]
		331 ± 2 [b]
K_m^{PEP} (μM)	36.3 ± 0.9	36.3 ± 1.1 [f]
		31.3 ± 0.4 [b]
Lactate dehydrogenase [e]		
V_m^{LDH} (U mg^{-1})	767 ± 9	768 ± 11 [f]
		771 ± 10 [b]
K_m^{NADH} (μM)	13.9 ± 1.3	14.0 ± 2.1 [f]
		26.2 ± 0.9 [b]
K_m^{pyr} (μM)	207 ± 3	207 ± 5 [f]
		229 ± 7 [b]
K_i^{NADH} (μM)	17.0 ± 0.9	16.9 ± 1.5 [f]
		15.8 ± 1.3 [b]
Glutamate dehydrogenase [g]		
k_1 (μM^{-1} s^{-1})	20.2 ± 0.16	21.3 ± 0.19 [h]
k_2 (s^{-1})	11.9 ± 2.0	12.1 ± 2.2 [h]
k_3 (s^{-1})	29.8 ± 2.0	31.5 ± 2.5 [h]
k_4 (s^{-1})	63.7 ± 6.0	70.6 ± 7.6 [h]
k_5 (s^{-1})	5.89 ± 0.33	6.13 ± 0.34 [h]

[a] Literature values from Pike and Duggleby [11].
[b] Determined from initial velocity measurements.
[c] Calculated from rates of enzyme inactivation.
[d] Analysis of residual substrate concentrations.
[e] Literature values from Duggleby [15].
[f] Determined by progress curve analysis.
[g] Literature values from Chandler et al. [14].
[h] Determined from pre-steady state kinetic measurements.

The fitted curves (Fig. 3) are in excellent agreement with the data.

Some of the progress curves for the pyruvate kinase/lactate dehydrogenase system are shown in Fig. 3. The fitted parameters are shown in Table 2 and again it is seen that these show little difference from the literature values. The fitted curves (Fig. 3) are in excellent agreement with the data.

The transient-state kinetics of glutamate dehydrogenase are illustrated in Fig. 4 and the results of analyzing these data are presented in Table 2. While there are some small variations between the literature values and those obtained here, such as a 10% difference in the value of k_4, this is undoubtedly due to inaccuracies in measuring the data from the published graph. The fitted curves provide a very good description of the data.

5. Discussion

Initially some simulated data were generated; these constituted an important test of the procedure because

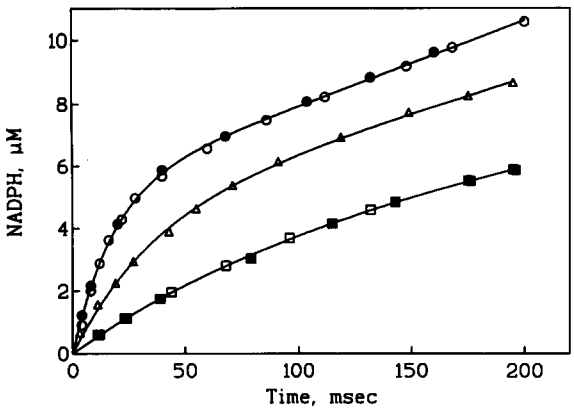

Fig. 4. Transient-state kinetics of the reaction catalyzed by glutamate dehydrogenase. The initial concentration of $NADP^+$ was 1250 μM (in duplicate), 240 μM or 80 μM (in duplicate). Other conditions were as described in the next.

they represent the only objective measure of whether the analysis produces the correct values. This is because the equation used to generate the data (Eq. (10)) and those used to fit them (Eqs. (1) and (2)) were different, although each is a representation of the same underlying model (Scheme 1) when j_1 and j_2 are equal. As shown by the results in Table 1, the values obtained did not differ from the theoretical values. Thus the analysis of progress curves by this combined numerical integration and non-linear regression program is a reliable procedure.

Next the analysis was applied to an experimental system, alkaline phosphatase. As shown for the curves in Fig. 2, which were all obtained at an initial substrate concentration of 10 mM, it is clear that each reaction ceases well before total exhaustion of the substrate. This is due to progressive enzyme inactivation and, in accord with the relevant theory [10], the residual substrate concentration decreases as the initial enzyme concentration increases. The published analysis of these data [11] used the residual substrate concentrations to estimate j_1 only. The other kinetic parameters (k_3, K_a and K_p) had to be obtained independently. In the present analysis, all four parameters could be obtained simultaneously from one experiment and the values obtained were in excellent agreement with those published previously. Moreover, it was shown by the appropriate statistical analysis that both the enzyme-substrate and the enzyme-phosphate complex were stable under these experimental conditions.

The second experimental system analyzed was the coupled reactions catalyzed by pyruvate kinase and lactate dehydrogenase. Examination of the data (Fig. 3) reveals a distinct lag in NAD^+ formation. This is because each of the enzymes is present at similar activities and the formation of the final product will reflect the kinetics of both reactions. This is not the normal method for performing coupled reactions where it is usual that the activity of the second enzyme in the sequence would be vastly in excess of that of the first. These particular data were obtained as a model for the normal metabolic situation where none of the enzymes is in huge excess, and provided a useful test of the present procedure. The fitted parameters obtained were in excellent agreement with the previous analysis of the same data and corresponded well to values determined from independent experiments.

It is worth noting here that the previous analysis of the pyruvate kinase/lactate dehydrogenase system used CRICF [14], a Fortran program written for mainframe computers that also combines numerical integration with non-linear regression. Other programs that achieve similar results have also been described [17–19]. The advantage of DNRP-RKF is that it runs on an IBM-compatible personal computer and provides a very simple way to define any particular set of equations (see Fig. 1). However, it might have been expected that the previous analysis using CRICF and present analysis would yield identical results. The reason for the differences is that data analyzed were slightly different; the original data files are no longer available and the present data set was reconstructed from laboratory notebooks.

There are many biochemical systems described by differential equations that cannot be integrated and the most common solution to this problem is to differentiate the data (measure rates). However, this approach will often obscure important properties of the system. For example, Scheme 1 includes provision for instability of a transitory enzyme complex (EA) and the only way that this complex can be observed is while catalysis is proceeding. Thus one is led naturally to *observing* progress curves, and it is desirable to be able to *analyze* such curves as well. The final system studied here, the transient-state kinetics of glutamate dehydrogenase, is an example of a situation where rate measurements are virtually meaningless. By analyzing the progress curves it is possible to estimate all of the rate constants that describe this system (Scheme 1).

There are a number of other possible situations where the type of analysis described here may prove useful. For example, it is known that a number of compounds act as slow-binding enzyme inhibitors [20]. The slow onset of inhibition is best studied by following progress curves but this should be done under conditions where substrate depletion is insignificant. This may necessitate high concentrations of substrate that tend to obscure the very inhibition that one wishes to observe. The present approach offers a facile solution to this problem that will allow the progress curves for slow-binding enzyme inhibitors to be analyzed even when there is considerable substrate depletion.

6. Acknowledgement

This work was supported by the Australian Research Council.

7. References

[1] Orsi, B.A. and Tipton, K.F. (1979) Methods Enzymol. 63, 159–183.
[2] Nimmo, I.A. and Atkins, G.L. (1974) Biochem. J. 141, 913–914.
[3] Fernley, H.N. (1974) Eur. J. Biochem. 43, 377–378.
[4] Duggleby, R.G. and Wood, C. (1989) Biochem. J. 258, 397–402. [Correction (1990) 270, 843.]
[5] Boeker, E.A. (1984) Biochem. J. 223, 15–22.
[6] Boeker, E.A. (1984) Experientia 40, 453–456.
[7] Boeker, E.A. (1985) Biochem. J. 226, 29–35.
[8] Segel, I.H. (1975) in Enzyme Kinetics, pp. 506–749, Wiley, New York.
[9] Selwyn, M.J. (1965) Biochim. Biophys. Acta 105, 193–195.
[10] Duggleby, R.G. (1986) J. Theor. Biol. 123, 67–80.
[11] Pike, S.J. and Duggleby, R.G. (1987) Biochem. J., 244, 781–785.
[12] Stoer, J. and Bulirsch, R. (1980) in Introduction to Numerical Analysis, pp. 410–429, Springer, New York.
[13] Duggleby, R.G. (1984) Comput. Biol. Med. 14, 447–455.
[14] Chandler, J.P., Hill, D.E. and Spivey, H.O. (1972) Comput. Biomed. Res. 5, 515–234.
[15] Duggleby, R.G. (1983) Biochim. Biophys. Acta 744, 249–259.
[16] Ellis, K.J. and Duggleby, R.G. (1978) Biochem. J., 171, 513–517.
[17] Holzhütter, H.G. and Colosimo, A. (1990) Comput. Appl. Biosci. 6, 23–28.
[18] Eberhard, M. (1990) Comput. Appl. Biosci. 6, 213–221.
[19] Zimmerle, C.T. and Frieden, C. (1989) Biochem. J. 258, 381–387.
[20] Morrison, J.F. and Walsh, C.T. (1988) Adv. Enzymol. Relat. Areas Mol. Biol. 61, 201–301.